Environment Canada

Environnement Canada

National Water Research Institute

Institut National de Recherche sur les Eaux

NWRI Contribution 84-40
Beltaos (24)
Wong (05)
Study 83-314

DOWNSTREAM TRANSITION OF RIVER ICE JAMS

by

S. Beltaos[1] and J. Wong[2]

[1]Research Scientist
[2]Research Engineer
Environmental Hydraulics Section
Hydraulics Division
National Water Research Institute
Canada Centre for Inland Waters

March 1984

ABSTRACT

The granular mass theory of river ice jams is extended to their downstream transition as a means of improving understanding of conditions at jam toes. The theory is coupled with the equations of motion under, and seepage through, the jam and the resulting differential equations are solved numerically. The present model applies to wide rectangular channels and involves several coefficients whose precise values in nature are unknown. Example calculations are performed to illustrate the sensitivity of the model to the various coefficients. Preliminary application of the model to two case studies resulted in plausible findings with regard to grounding of ice jams.

RESUME

La théorie de la masse granulaire des embâcles de rivières est étendue à leur transition à l'aval à titre de moyen permettant d'améliorer la compréhension des conditions aux pieds des embâcles. La théorie est associée aux équations du mouvement sous les embâcles et de l'infiltration au travers de ces derniers, et les équations différentielles résultantes sont résolues numériquement. Le présent modèle s'applique aux larges chenaux rectangulaires et fait intervenir plusieurs coefficients dont la valeur précise dans la nature n'est pas connue. Des calculs sont exécutés à titre d'exemple afin d'illustrer la sensibilité du modèle à ces divers coefficients. L'application préliminaire du modèle à deux études de cas a donné des résultats plausibles quant à l'échouage des embâcles.

MANAGEMENT PERSPECTIVE

In order to deal with problems associated with river ice jams such as predicting flood levels or removing destructive jams, it is necessary that the mechanics of ice jamming be fully understood. Up to now there are no theories capable of dealing with the downstream portion of the jam where the water surface slope and jam thickness increase rapidly. In this report, a method is proposed for the calculation of the jam configuration in this transition region. Although the model applies to very wide rectangular channels only, it represents a significant advance as it is the first model capable of calculating the jam configuration in the downstream toe region.

Y.L. Lau, A/Chief
Hydraulics Division

PERSPECTIVE DE GESTION

Pour être en mesure de résoudre les problèmes associés aux embâcles de rivières, comme la prévision des niveaux des crues ou la suppression des embâcles destructifs, il est nécessaire de comprendre parfaitement la mécanique de la formation des embâcles. Jusqu'ici il n'existait aucune théorie traitant de la partie aval des embâcles où la pente de la surface de l'eau et l'épaisseur de glace augmentent rapidement. Le présent rapport propose une méthode permettant de calculer la configuration de cette zone de transition de l'embâcle. Quoique le modèle ne s'applique qu'à des chenaux rectangulaires très larges, il marque un progrès important puisqu'il est le premier permettant de calculer la configuration dans la zone du pied à l'aval d'un embâcle.

Y.L. Lau, Chef intérimaire
Division de l'hydraulique

INTRODUCTION

A major consequence of ice cover formation on northern rivers is the jamming that occurs during the spring breakup of the cover and, to a lesser degree, during the freeze-up period. Due to their large aggregate thickness and hydraulic resistance relative to those of sheet ice, jams tend to cause unusually high water stages. This has repercussions in many operational and design problems such as overturning moment on river structures due to moving ice, forces on ice booms, spring flooding and associated stage-frequency relationships, river bed scour due to surges from released jams, to mention but a few.

At present, complete mathematical simulation of water stages during breakup is only a hope for the future. There are simply too many unknowns: it is not known whether, where, and when a jam will form. Even if it is assumed that a jam has been initiated at a specified location, it is not known exactly what occurs at the toe (downstream end) and thus it is not possible to formulate an appropriate boundary condition for the jam's subsequent evolution; and even if the configuration of an ice jam at a specified time is given or assumed, it is not known how, why, and when the jam will release.

Faced with such difficulties, research has concentrated on the relatively simple problem of equilibrium jams, i.e., jams that no longer evolve. This approach has considerable practical merit since it can be argued that, under certain circumstances, the highest water stages occur when a jam has attained equilibrium. Theoretical work has resulted in a model for floating jams in equilibrium that has been tested with some success versus experimental results. Virtually nothing is known, however, about grounded (otherwise known as "dry") jams. Fig. 1 gives a schematic illustration of an equilibrium jam. In Fig. 1 it has been assumed that the jam was initiated at the edge of an undisturbed ice sheet and attained a steady-state condition. Typically, there are three regions within the length of such a jam:

1. Upstream transition: For a certain distance below the head of the jam, the thickness increases and approaches an asymptotic value. The flow under the jam is of the gradually varied type. This should be the case for jams of the "wide channel" kind which represent a very common occurrence (see also pertinent measurements in Ref. 5).
2. Equilibrium reach: The thickness of the jam is relatively uniform and approximately equal to the asymptotic value mentioned earlier. This value has been termed the equilibrium thickness (14, 15). The flow under the jam is uniform and the water surface slope is equal to the channel bed slope, S_o. This concept applies to prismatic channels but may be extrapolated to natural streams by replacing S_o with the open-water surface slope, provided: (1) the reach under consideration is long enough to permit meaningful averaging of channel characteristics; and (2) the flow is free to assume a uniform condition, i.e., there are no significant control effects in the reach of interest.
3. Downstream transition: Below the equilibrium reach, the water surface profile steepens progressively to meet the relatively low water stage that prevails at the toe of the jam (e.g., see Refs. 2, 7, 8, 9). The jam and flow configurations in this region are difficult to assess and could vary depending on local conditions and mode of jam initiation.

It should be recognized that the type of jam depicted in Fig. 1 occurs often but is by no means universal. If the jam is too short, the equilibrium thickness region may not exist, while in reaches that are strongly influenced by controls (e.g., river mouths) uniform flow may not occur under the jam.

To date, research has concentrated on predicting ice jam thickness and stage in the equilibrium reach with a satisfactory measure of success (4, 6, 13, 15). At the same time, it is recognized that the downstream transition plays an important role in many applications. These include conditions for grounding of ice jams; and design of

measures to prevent or remove destructive jams (depends on understanding of toe conditions).

Existing knowledge is utilized herein to develop a preliminary method for calculating ice jam and flow characteristics in the downstream transition. Because the numerical values of the coefficients utilized in this study are unknown, a sensitivity analysis is performed to identify those coefficients that have a significant impact on prediction and obtain preliminary understanding of the ranges within which the predicted parameters are expected to vary. Future research requirements are discussed.

2.0 BACKGROUND INFORMATION

A review of theoretical developments on river ice jams has been presented in Ref. 4, along with a verification based on numerous case studies. The theory treats an ice jam as a floating granular mass that attains a thickness adequate to withstand the applied forces. For a very wide rectangular channel and a laterally uniform and cohesionless jam, this condition leads to (14,15 with modification):

$$\frac{dt_s}{dx} = \beta_1[\beta_2 \frac{fo\ q^2}{4gh^2 t_s} + S_w] - \beta_3 \frac{t_s}{W} \qquad (1)$$

in which t_s = submerged portion of ice jam thickness; g = acceleration due to gravity; h = depth of flow under the jam; q = discharge per unit width of the flow under the jam; S_w = slope of water surface; W = channel width; and

$$\beta_1 = \frac{s_i^2 \gamma_w}{2K_x \gamma_e} \qquad (2)$$

$$\beta_2 = \frac{f_i}{2f_o} \tag{3}$$

$$\beta_3 = \frac{C_o}{K_x} \tag{4}$$

where s_i = specific gravity of ice; γ_w = unit weight of water; f_i = friction factor of the jam underside; and f_o = composite friction factor of the flow under the jam. Moreover,

$$\gamma_e = 0.50\ (1 - s_i)(1 - p)\ s_i \gamma_w \tag{5}$$

in which p = porosity of the jam. The dimensionless coefficients C_o and K_x define strength characteristics of the jam, i.e., C_o is the ratio of frictional strength (that develops at the sides of the jam) to the thickness-averaged, effective, vertical stress $\sigma_y (= \gamma_e t)$; and K_x is the ratio of the compressive strength of the jam to σ_y.

In the equilibrium reach, $dt_s/dx = 0$, so that Eq. 1 provides a means of computing the equilibrium thickness of the jam. This relationship can be coupled with a hydraulic resistance equation to determine the equilibrium flow depth and the total water depth, using the relationship (see Fig. 1).

$$H = h + t_s \tag{6}$$

Inspection of Eqs. 1 to 5 suggests that the equilibrium parameters H_e, t_{se}, and h_e (the suffix "e" is used to denote equilibrium conditions) are independent of K_x and depend on the product $C_o(1-p)$. The latter is better known in the literature as μ. For equilibrium conditions, the theoretical expression for H_e is (4):

$$\frac{H_e}{WS_o} \equiv n = 0.63\, f_o^{1/3}\, \xi + \frac{5.75}{\mu}\left[1 + \sqrt{1+0.11\mu f_o^{1/3}\left(\frac{f_i}{f_o}\right)\xi}\right] \quad (7)$$

in which ξ is a dimensionless discharge parameter:

$$\xi \equiv \frac{(q_e^2/gS_o)^{1/3}}{WS_o} \quad (8)$$

Note that in Eq. 7, the first term on the RHS represents h_e/WS_o and the second term represents t_{se}/WS_o.

As outlined in (4), only n and ξ are measurable in nature owing to lack of technology for insitu measurements of ice jam thickness during breakup. Fig. 2 shows data summarized in Refs. 2 and 4, plotted in the form of n versus ξ. While there is considerable scatter, probably caused by variations of the coefficients f_o, μ and f_i, a single line could be drawn through the equilibrium jam data points and used as a first approximation. Moreover, it was shown in (4) that values of ice jam thickness and thence of f_o, f_i, and μ, could be estimated using an indirect analysis. The latter utilizes hydraulic resistance data for winter jams that freeze in place and permit safe access (12). It was thus found that μ assumed fairly consistent values and averaged 1.20. The ratio f_i/f_o ranged from 0.63 to 1.64 and averaged 1.25 without showing any consistent trend with ξ. However, the composite friction factor, f_o, showed a consistent decrease with increasing ξ. This was considered plausible given that f_o would be expected to increase with increasing values of t_{se}/h while the latter occurs when ξ decreases. Based on this finding an "average" relationship between f_o and t_{se}/h was generated as follows. The values of μ and f_i/f_o were fixed at 1.20 and 1.25 respectively and Eq. 7 was used to compute the value of f_o corresponding to a given pair (ξ,n) taken from the "average" line of Fig. 2. With this, the

corresponding value of t_{se}/WS_o can also be calculated and t_{se}/h_e determined. In this manner a plot of f_o versus t_{se}/h_e was prepared for the range t_{se}/h_e = 0.2 to 2.0. The data points of this graph were fitted well by the equation

$$f_{oe} = 0.507\ (t_{se}/h_e)^{1.17} \tag{9}$$

It is emphasized that, in reality, no unique relationship between f_o and t_{se}/h can be expected to exist because f_o also depends on channel bed characteristics. Eq. 9 is merely a convenient, "average" relationship that fits the "average" line of Fig. 2 when used in conjunction with Eq. 7 and average values of μ and f_i/f_o.

To date, seepage flow through the voids of jams has been neglected and this does seem to be realistic for equilibrium conditions given the good performance of the equilibrium theory. However, when the downstream transition is considered, the seepage flow can no longer be ignored because the transition may entail grounding of the jam where the entire discharge must flow as seepage. The results reported in Ref. 16 suggest that seepage through ice jam voids should be of the non-laminar type, i.e.,

$$q_p = \lambda t_s \sqrt{S_w} \tag{10}$$

in which q_p = seepage flow discharge per unit width; and λ = dimensional coefficient such that $\lambda\sqrt{S_w}$ = apparent seepage velocity (m/s). Laboratory tests with polyethylene blocks (5.08 x 5.08 x 0.635 cm and 10.16 x 10.16 x 1.27 cm) have indicated that (Beltaos and Wong, Unpublished Data)

$$\lambda = \sqrt{\frac{Kp^3}{1-p}\ gd_s} \tag{11}$$

in which K = dimensionless coefficient = 0.3 - 0.7, depending on block orientation within the jam; and $d_s = 6/M_s$ with M_s = specific

surface = surface area per unit volume of the particles of the porous medium (Eq. 11 is essentially the Ergun formula, as quoted in Ref. 1). It is not known whether Eq. 11 can be extrapolated to natural ice jams where the ice blocks are neither parallelepiped nor uniform in shape and size. To obtain an order-of-magnitude estimate, put h_i = ice block thickness = 0.5 m and assume circular ice blocks with average diameter of 2.0 m. Then Eq. 11 gives λ = 0.8 - 1.2 m/s for p = 0.4 and λ = 1.8 - 2.7 m/s for p = 0.6 for the range of K values given above. If q_e is the flow discharge under an equilibrium jam, it can be shown that

$$\frac{q_{pe}}{q_e} = \frac{\sqrt{f}_{oe}}{2} \frac{t_{se}}{h_e} \frac{\lambda}{\sqrt{gh_e}} \tag{12}$$

which, for jams that are not excessively thick, indicates that q_{pe}/q_e would be generally less than 0.10. This tentatively justifies the neglect of seepage in previous applications.

3.0 ANALYTICAL CONSIDERATIONS

3.1 Assumptions

The simple case of a very wide rectangular channel is considered. Consequently, it can be assumed that the jam thickness does not vary across the channel. Moreover, a steady state condition is assumed. It is recognized that the final configuration of the jam might be partly influenced by unsteady conditions that prevailed during earlier stages of its formation. There is no direct evidence to justify the assumption of steady state. However, this assumption has been implicit in all literature regarding equilibrium conditions without noticeable adverse effects. Moreover, it is known that unsteadiness is most intense during surge-like phenomena caused by releases of major ice jams (3,10). Near the surge front, the flow discharge can be much larger than that of the incoming flow far upstream of the initial

location of the jam. However, the moving ice lags well behind the front and is associated with a more moderate flow discharge. When the ice run is arrested and a new jam begins to form, the discharge under the new jam is further reduced by the rate of storage upstream of the edge of the jam where water levels increase rapidly. In addition, and with reference to the equilibrium reach, Beltaos (4) has shown that the theory would still provide acceptable results (with regard to H) even where the jam forming discharge is as much as twice that which prevails during the steady state condition after the jam has formed. These considerations may explain the success of the steady-state assumption, though proof can only be furnished by development of a capability to model the unsteady jam formation process.

3.2 Continuity

Since a steady state condition has been assumed, the total discharge, q_T, is independent of the downstream distance, x; hence

$$q_T = q + q_p = q + \lambda t_s \sqrt{S_w} = \text{const.} \qquad (13)$$

3.3 Momentum

It can be shown that integration over the flow depth of the momentum equation in the x-direction gives

$$\rho\left[\frac{d}{dx}(qV) - V_h\frac{dq}{dx}\right] = \rho g h S_w - (\tau_i + \tau_b) \qquad (14)$$

in which the one-dimensional approximation, $\int_0^h u^2 dy \approx qV$, has been made [u = flow velocity in x-direction; y = coordinate perpendicular to channel bed]; ρ = density of water; V = average flow velocity = q/h; V_h = value of u at the jam underside; and τ_i, τ_b are flow shear

stresses on jam underside and channel bed respectively. [In Eq. 14 and also in Eq. 1, mentioned earlier, the cosines of small angles are assumed to be equal to one.]

The velocity V_h is unknown. As a first approximation, it is assumed that

$$V_h = \alpha V; \ \alpha = \text{const.} \tag{15}$$

Substituting Eq. 15 in Eq. 14 and re-arranging, gives

$$(1-\alpha)\ \rho V^2 \frac{dh}{dx} = \rho g h \left[S_w - (2-\alpha) \frac{d}{dx} \left(\frac{V^2}{2g}\right)\right] - (\tau_i + \tau_b) \tag{16}$$

in which $\tau_i + \tau_b$ may also be written as

$$\tau_i + \tau_b = \frac{f_o}{4} \rho V^2 \tag{17}$$

If seepage were negligible, Eq. 13 would give $dq/dx = 0$ whereby Eq. 14 would reduce to the gradually varied flow equation. The same expression would be obtained if V_h were taken as equal to V (substitute $\alpha = 1$ in Eq. 16).

Putting $V = q/h$ and considering the velocity head gradient, $\frac{d}{dx} \left(\frac{V}{2g}\right)^2$, gives after some algebra and use of Eq. 13:

$$\frac{dq_p}{dx} = - \frac{gh^2}{q} \frac{d}{dx} \left(\frac{V^2}{2g}\right) - \frac{q}{h} \frac{dh}{dx} \tag{18}$$

Differentiating Eq. 10 and re-arranging gives

$$\frac{dS_w}{dx} = \frac{2}{t_s} \left[\frac{\sqrt{S_w}}{\lambda} \frac{dq_p}{dx} - S_w \frac{dt_s}{dx} \right] \tag{19}$$

Substituting Eq. 18 in Eq. 19 and using Eqs. 16 and 17 gives after some manipulation:

$$\frac{dS_w}{dx} = \frac{2\sqrt{S_w}}{(2-\alpha)t_s}\left\{\frac{q}{\lambda h}\frac{f_o}{4} - \frac{q}{\lambda h}\frac{dh}{dx} - \frac{S_w g h^2}{\lambda q} - (2-\alpha)\sqrt{S_w}\frac{dt_s}{dx}\right\} \quad (20)$$

Moreover, by the definition of S_w:

$$\frac{dh}{dx} = S_o - S_w - \frac{dt_s}{dx} \quad (21)$$

Eqs. 1, 20 and 21 form a group of three first-order ordinary differential equations with, essentially, three unknowns, h, t_s and S_w. Note that q can be expressed in terms of S_w and t_s using Eq. 13 while f_o can be related to ice jam and channel bed resistance characteristics (4).

3.4 Boundary Condition

The preceding analysis has shown that the downstream transition profile would be completely specified if an appropriate boundary condition were given. In applications, the obvious boundary condition would be at the toe of the jam where H_t, the local value of H is usually known or can be estimated. However, the local values of S_w and t_s are unknown and practically impossible to measure. Thus, if computation were to start at the toe and proceed upstream, an extremely laborious, trial-and-error procedure would be necessary, i.e., guess t_s and S_w at toe; compute ice jam profile and check whether there exists asymptotic convergence to the equilibrium parameters S_o, h_e and t_{se} (these can be determined independently using the equilibrium theory).

A less straighforward but more practical approach is to start from the equilibrium reach and proceed downstream. In this manner, the downstream transition configuration can be calculated, independently of

H_t, until grounding occurs (h = 0), as sketched in Fig. 3. The value of H_t may also be plotted in Fig. 3 to determine the toe location and condition. If $H_t > H_g$ (= value of H at the location of grounding), the toe will be of the floating type as shown in Fig. 3. However, if $H_t < H_g$, the jam will ground for a distance dictated by H_g, H_t, λ and q_T (see also later discussion).

3.5 Coefficients

Inspection of Eqs. 1, 20 and 21 suggests that the solution depends on several coefficients, e.g., α, f_o, β_1, β_2, β_3 and λ.

The coefficient α relates to the velocity at the jam underside, V_h, expressed as a fraction of the average flow velocity, V. While V_h must be non-zero to enable progressive increase of q_p, leading to eventual grounding with $q_p = q_T$, it is plausible to expect that α should be less than one. Thus two values of α have been tried, $\alpha = 0$ and $\alpha = 1$.

The composite friction factor f_o should, ideally, be related to ice jam and channel bed resistance characteristics. While this can be done in a number of ways (e.g., see Ref. 4), it was thought preferable for the present exploratory study to use the relatively simple empirical relationship mentioned earlier (Eq. 9), i.e., put

$$f_o = c(t_s/h)^m; \; c = 0.507; \; m = 1.17 \tag{22}$$

Using Eqs. 2 and 5, β_1 can be expressed as

$$\beta_1 = s_i/K_x(1-s_i)(1-p) \tag{23}$$

For ice jams, $s_i = 0.92$ while a value of $p = 0.4$ is often assumed. The main unknown is K_x. It has been suggested (14) that, for a cohesionless jam:

$$K_x = \tan^2\left(\frac{\pi}{4} + \frac{\phi}{2}\right) \tag{24}$$

in which ϕ = angle of internal friction of the jam. Comparing the theories of (13) and (15) results in:

$$\tan\phi \tan^2\left(\frac{\pi}{4} + \frac{\phi}{2}\right) = \frac{\mu}{(1-p)K_1} \tag{25}$$

in which K_1 = coefficient of lateral thrust. According to Ref. 13, $K_1 \leq 1$ depending on the active or neutral state of the granular mass of the jam. Moreover, β_3 becomes (using Eq. 4)

$$\beta_3 = \frac{\mu}{(1-p)K_x} \tag{26}$$

For $p = 0.4$, Eq. 25 can be solved for different values of K_1 and thus ϕ, K_x, β_1 and β_3 calculated, as shown in Table 1. It may be noticed in Table 1 that a realistic range for K_1 is 0.20 to 1.00 because below K_1 = 0.2, ϕ becomes implausibly large. Thus, the range 3.2 to 10.0 has been considered for K_x.

The coefficient β_2 is the ratio $f_i/2f_o$ which, from Ref. 4, has been taken in the range 0.3 to 0.8 with an average value of 0.625.

The seepage parameter λ is also unknown for natural ice jams. Based on earlier discussion, the range 0.75 m/s to 5.0 m/s has been considered.

4.0 NUMERICAL SOLUTION

As mentioned earlier, the solution proceeds from the equilibrium reach in the downstream direction. However, inspection of Eqs. 1, 20 and 21 shows that all gradients vanish at equilibrium so that the numerical algorithm cannot be started in a simple manner. The following approach is thus adopted to circumvent this difficulty (see

also Ref. 14). At a location arbitrarily designated by $x = 0$, let t_s be set equal to $t_{se} + \Delta t_s$ where Δt_s is a small increment. If appropriate values can be determined for the corresponding ΔS_w and Δh, a set of values for t_s, h and S_w at $x = 0$ can be generated which would enable computation to start since the respective gradients will no longer be zero. To calculate Δh and ΔS_w, put

$$\Delta h = \psi \, \Delta t_s \tag{27}$$

$$\Delta S_w = \theta \, \Delta t_s \tag{28}$$

in which $\psi = (dh/dt_s)_e$ and $\theta = (dS_w/dt_s)_e$ with the suffix "e" denoting equilibrium values. Moreover, it is noted that

$$\psi = \left(\frac{dh}{dt_s}\right)_e = \frac{(dh/dx)_e}{(dt_s/dx)_e} = \frac{0}{0} \tag{29}$$

which is indeterminate. Utilizing L' Hospital's rule:

$$\psi = \frac{\left[\frac{d}{dt_s}\left(\frac{dh}{dx}\right)\right]_e}{\left[\frac{d}{dt_s}\left(\frac{dt_s}{dx}\right)\right]_e} \tag{30}$$

Similar considerations apply to S_w. This approach leads to rather laborious algebra and was simplified as follows.

It is assumed that, near the equilibrium reach, f_o remains constant ($= f_{oe}$) since t_s and h change very little. Moreover, it can be shown that the velocity head gradient is much smaller than the water surface slope, while $\rho V^2(dh/dx) \ll \tau_i + \tau_b$. Hence, Eq. 16 (with Eq. 17) reduce to

$$S_w = \frac{f_o q^2}{4gh^3} \tag{31}$$

It can be shown further that, near equilibrium, q changes very little so that Eq. 31 can be reduced to

$$S_w = S_o \, (h/h_e)^{-3} \tag{32}$$

These assumptions lead to a quadratic equation for ψ, as outlined in Appendix III. With this simplification, a value of Δt_s is selected and Δh is calculated from Eq. 27 which enables determination of h at x = 0. The value of S_w at x = 0 is found from Eq. 32.

The three ordinary differential equations (Eq. 1, 20 and 21) can now be solved by numerical methods. The initial-value problem is solved by an algorithm which utilizes the Runge Kutta-Verner Fifth and Sixth Order Method. In the algorithm, the step size, Δx, is reduced when the change in the value of h or t_s exceeds a certain tolerance value. Therefore, the step size is initially set to a standard value of 50 m at x = 0 and becomes smaller as the toe of the jam is approached and the values of h and t_s change more significantly. Test runs have shown that reducing the initial step size Δx did not significantly affect the final solutions obtained for the examples considered herein.

The algorithm produces a table with values of x, h, t_s, and S_w. Eventually, grounding occurs (i.e., h = 0) and the computation is terminated. The algorithm is coded in the computer program, NAME, which was developed by the writers and is available at the Hydraulics Division, National Water Research Institute. The program (a) determines the conditions in the equilibrium reach of the ice jam; (b) determines the initial conditions in the downstream transitional stage; and (c), solves the differential equations which govern the downstream transition.

The Runge Kutta-Verner Fifth and Sixth Order Method was coded in a routine called DVERK and is available in the International Mathematical and Statistical Libraries (Ref. 11).

Several runs were made using the simplified method for starting the computation. It was found that the coefficient α (set equal to zero and one) hardly affected the results. Convergence was tested by changing the value of Δt_s and showing that this did not affect the results so long as $\Delta t_s \ll t_{se}$.

If the above described assumptions to simplify the starting of the computation are not invoked, a more elaborate analysis is required to simultaneously solve for ψ and θ, as explained in Appendix III. While this may have a large effect on ψ, it was found that there were insignificant differences in the computed values of h, t_s, and S_w relative to those computed by the simplified method. However, there were significant differences in x_g, the distance from the origin to the point of grounding. This is considered a minor discrepancy because x_g is largely arbitrary owing to the asymptotic nature of the solution as equilibrium is approached. Thus the final series of runs were made using the approximate method and putting $\alpha = 0$.

5.0 RESULTS

Two examples, intended to simulate known natural events were selected, i.e.,

(a) $W = 109$ m and $S_0 = 0.00027$. This refers to an ice jam observed in the Thames River (Ontario) near the mouth, on February 22, 1981(2). It is not known whether this jam was in equilibrium though it remained stable for several hours. In addition, the discharge is also unknown because there was flooding upstream of the jam so that it is estimated that $q_T < 4$ m^2/s. Despite these uncertainties, this example was chosen for analysis because of the strong evidence of grounding near the toe (very steep water surface

slope near toe-over 0.004 in the last 80 m of the jam profile; and large local accumulations of broken ice, rising well above the water surface which by a simple flotation calculation suggests grounding). The value S_o = 0.00027 was assumed, as a first approximation, to be equal to the water surface slope far upstream of the toe.

(b) W = 560 m and S_o = 0.00036. This refers to the Athabasca River near Fort McMurray (Alberta) where observations over several years (7,8,9) have indicated very frequent jamming and grounding near the toe. The value of q_T during the spring breakup is usually in the range 2-4 m^2/s. The above noted values of W and S_o apply to the 1977 ice jamming events (Ref. 7 and personal communication) and depend on the location of the jammed reach. For example, upstream of the reach considered herein, the river narrows to 430 m and steepens to 0.00055 (Andres, pers. comm.) A series of computational runs were also made for the latter values but the results did not alter the findings with regard to grounding.

Figures 4 and 5 show typical calculated transition profiles while Tables 2 and 3 summarize the main results. It is noteworthy that most of the change in t_s and H occurs near the toe where, in addition, water surface slopes become extreme. The values of S_w over the last 100 m and 200 m of the jam profile appear realistic in comparison with what is observed in nature (2,7,8,9).

The effects of λ and K_x on H_g are illustrated in Fig. 6. While H_g decreases somewhat with increasing λ, K_x has a more pronounced effect and H_g decreases considerably when K_x increases. This implies that increasing values of K_x (and thus increasing ϕ-Table 1) reduce the likelihood of grounding. Figure 7 shows that increasing values of β_2 ($\equiv f_1/2f_o$) cause H_g to increase while Fig. 8 indicates that x_g increases with increasing K_x and λ.

For the Thames River example, the value of q_T that best reproduces the assumed equilibrium portion of the profile is estimated as 3.09 m^2/s. For λ = 0.75 m/s and β_2 = 0.625, H_g is 4.86 m for K_x = 3.23; 4.30 m for K_x = 8.00; and 4.13 m for K_x = 10.00. For λ = 5m/s, these values become 4.72, 4.15 and 3.98 m. Given that the value of H_t was 4.30 m, it appears that the numerical calculation indicates grounding except for very large λ's and K_x's. In Table 4, values of H_g and H_t are tabulated versus q_T. It is seen that, for K_x = 4.32, the jam toe would remain grounded even for as large a value of q_T as 6.0 m^2/s. For K_x = 8.00, the toe would become of the floating type for $q_T \geq 3.09$. Thus, it would appear that increasing discharge reduces the likelihood of grounding in this instance.

Table 5 gives similar results for the Athabasca River example where grounding is indicated regardless of q_T and K_x (λ = 0.75 m/s; β_2 = 0.625).

6.0 APPROXIMATE CALCULATION OF H_g

In cases where only an estimate of H_g is required, a good approximation can be obtained without resort to the full numerical solution. This can be accomplished by considering t_s as a function of h and examining properties of this function in the limiting cases of grounding and equilibrium. The result is the following approximate relationship (see Appendix IV for details):

$$H_g' = t_{se} + \frac{h_e}{3}\left(\frac{2\beta_1}{1+\beta_1} + \frac{1}{|\psi|}\right) \qquad (33)$$

in which H_g' is the approximate value of H_g and ψ is calculated by the detailed method.

Comparisons of Eq. 33 with the values of H_g obtained by the numerical solution are summarized in Table 6 where the error is seen to be less than 8%. In general, the error increases in absolute value with increasing difference between the quantities $\beta_1/1+\beta_1$ and $1/|\psi|$.

7.0 DISCUSSION

The preceding analysis has indicated that the preliminary calculation method described herein is realistic, at least in the sense that it predicted grounding, as observed in two case studies. At this point, however, a number of questions arise that indicate a need for further study.

We have seen that when $H_g < H_t$, the jam toe would be of the floating type and the local value of t_s can be determined by the procedure illustrated in Fig. 3. However, it is not clear how the jam is held in place. Preliminary calculation has shown that a configuration such as sketched in Fig. 9 could quickly dissipate the thrust of the jam through additional friction that becomes available at the ice sheet-broken ice interface. Under such conditions, removal of an ice jam could be accomplished by breaking or causing to move the ice sheet that retains the jam.

When $H_g > H_t$, the jam toe would be grounded over a distance L_g given by (16)

$$L_g = \frac{\lambda^2(H_g^3 - H_t^3)}{3q_T^2} \qquad (34)$$

For $\lambda = 0.75$ m/s, $q_T = 2.0 m^2/s$ and $K_x = 4.32$, the data from Table 5 can be substituted in Eq. 34 to find $L_g = 17$ m which appears to be too short relative to what is observed in nature. One reason for this may be that λ has a larger value in the grounded portion than does in the

floating portion owing to less intense packing and thence higher p (see Eq. 11). For example, if λ were 2 m/s, the value of L_g would increase from 17 m to 121 m. It should also be pointed out that no natural stream has rectangular cross-section as assumed herein. The width decreases with decreasing stage so that complete grounding would require zero width. However, inspection of Eq. 1 suggests that this cannot occur because dt_s/dx will vanish (i.e., t_s will cease to increase) before W becomes zero. Thus, in a prismatic channel of plausible, non-rectangular geometry, the ice jam plan view would be expected to appear as sketched in Fig. 10.

While complete grounding seems to be, in a strict sense, impossible, conditions of "practically grounded" jams are conceivable. This would entail situations where the seepage discharge and area become much larger than those of the unobstructed flow under the jam. Development of a numerical computation scheme that will allow for variable width is now in progress as a means of studying grounding conditions in more detail.

Where a jam is strictly or practically grounded for a certain distance, L_g, it is difficult to even speculate on means for its removal. The stability of the jam would partly depend on friction characteristics between the channel bed and the accumulation of broken ice as well as on the thickness of the jam within the length L_g. It is conceivable that a jam would remain stable even in the absence of sheet ice downstream of the toe. In such instances, use of explosives might be ineffective if L_g and W are large; a means of raising the local water level could then be a possible remedy.

At present, knowledge of the coefficients f_1, f_o, p, K_x and λ is far from satisfactory. The assumed relationships for f_1 and f_o are considered realistic so long as t_s/h is in the range 0.2 to 2.0. However, as the point of grounding is approached, t_s/h tends to infinity and there is no evidence to suggest that this extrapolation, made for illustration purposes herein, is valid. Laboratory studies of "very thick" jams (i.e., large t_s/h) would be helpful in this regard.

Similar studies would also help improve understanding with respect to p, λ and K_x but ultimately field verification will be required. Unfortunately, only the water level profile along a breakup ice jam can be measured in nature. One could try to "adjust" the various coefficients so as to match observed and predicted profiles but such calibration would be uncertain given the relatively large number of coefficients involved. On the other hand, if technology for remote measurement of ice jam thickness becomes available, confidence in calibration would increase because then the mathematical model would have to "match" not only the water level profile but also the thickness profile of the jam.

As mentioned earlier, the present analysis assumes that the cosines of small angles are equal to one. Specifically, the angle of interest has a tangent equal to -dh/dx and its cosine does remain very close to unity until about 1m upstream of the point of grounding. However, within the last 1 m or so of the computation, -dh/dx becomes so large that cosarctan(-dh/dx) deviates significantly from one. While this may have an effect on the local values of t_s and h, an approximate analysis has indicated that the effect on H_g is of the order of a few centimetres and thus could be ignored. The reason for this favourable circumstance is that, by the time the cosine becomes significantly different from one, the value of H is already close to H_g; errors made subsequently with regard to dH/dx contribute very little to H in terms of a percentage.

8.0 SUMMARY AND CONCLUSIONS

Using the granular mass theory of river ice jams along with momentum, continuity and seepage considerations, a numerical algorithm has been developed to predict jam and flow characteristics in the downstream transition. The present model applies to very wide rectangular channels under steady flow conditions and involves several coefficients of which the precise values are unknown. Example

calculations have been performed to illustrate the sensitivity of the model to the various coefficients. Preliminary applications to two case studies have resulted in plausible findings with regard to grounding of ice jams. In turn, this could find applications in the design of measures to prevent or remove destructive jams. Work is in progress to improve the model so as to account for width variations with stage which would improve understanding of conditions near the jam toe.

ACKNOWLEDGEMENTS

Review comments by Dr. B.G. Krishnappan, Dr. Y.L. Lau, Head of Environmental Hydraulics Section, and Dr. T.M. Dick, Chief of Hydraulics Division, are appreciated.

APPENDIX I

References

1. Bear, J. Dynamics of Fluids in Porous Media. American Elsevier Publishing Company, Inc., New York, 1972.
2. Beltaos, S. Ice Freeze Up and Breakup in the Lower Thames River: 1980-81 Observations. National Water Research Institute, Unpublished Report, Burlington, Canada, 1983.
3. Beltaos, S. and Krishnappan, B.G. Surges from Ice Jam Releases: A Case Study. Canadian Journal of Civil Engineering, Vol. 9, No. 2, pp. 276-284, 1982.
4. Beltaos, S. River Ice Jams: Theory, Case Studies, and Applications. Journal of Hydraulic Engineering, Vol. 109, No. 10, pp. 1338-1359, 1983.
5. Calkins, D.J. Physical Measurements of River Ice Jams. Water Resources Research, Vol. 4, No. 4, pp. 693-695, 1978.
6. Calkins, D.J. Ice Jams in Shallow Rivers with Floodplain Flow. Canadian Journal of Civil Engineering, Vol. 10, No. 3, pp. 538-548, 1983.
7. Doyle, P.F. Breakup and Subsequent Ice Jam at Fort McMurray. Internal Report SWE-77-01, Transportation and Surface Water Engineering Division, Alberta Research Council, Edmonton, Canada, 1977.
8. Doyle, P.F. and Andres, D.D. 1978 Breakup in the Vicinity of Fort McMurray and Investigation of Two Athabasca River Ice Jams. Internal Report SWE-78-05, Transportation and Surface Water Engineering Division, Alberta Research Council, Edmonton, Canada, 1978.
9. Doyle, P.F. and Andres, D.D. 1979 Spring Breakup and Ice Jamming on the Athabasca River near Fort McMurray. Internal Report SWE-79-05, Transportation and Surface Water Engineering Division, Alberta Research Council, Edmonton, Canada, 1979.

10. Henderson, F.M. and Gerard, R. Flood Waves Caused by Ice Jam Formation and Failure. Proc. IAHR International Symposium on Ice, Quebec, Canada, Fol. 1., pp. 277-287, 1981.

11. International Mathematical and Statistical Libraries Inc. The IMSL Library, Vol. 3, Houston, Texas, 1980.

12. Nezhikovskiy, R.A. Coefficients of Roughness of Bottom Surface on Slush-Ice Cover. Soviety Hydrology, American Geophysical Union, Washington, D.C., pp. 127-150, 1964.

13. Pariset, E., Hausser, R., and Gagnon, A. Formation of Ice Covers and Ice Jams in Rivers. Journal of the Hydraulics Division, ASCE. Vol. 92, No. HY6, pp. 1-24, 1966.

14. Uzuner, M.S. and J.F. Kennedy. Hydraulics and Mechanics of River Ice Jams. Iowa Institute of Hydraulic Research, Report No. 161, The University of Iowa, Iowa City, Iowa, 1974.

15. Uzuner, M.S. and J.F. Kennedy. Theoretical Model of River Ice Jams. Journal of the Hydraulics Division, ASCE, Vol. 102, No. HY9, proc. Paper 12412, pp. 1365-1383, 1976.

16. Wong, J., S. Beltaos, and B.G. Krishnappan. Laboratory Tests on Ice Jam Dynamics. Submitted for publication to the Canadian Journal of Civil Engineering.

APPENDIX II

Notation

The following symbols are used in this paper.

c = coefficient.

C_o = dimensionless coefficient defining the frictional strength of the jam.

d_s = characteristic length of particles of a porous medium = $6/M_s$.

e = subscript denoting equilibrium condition.

f_i = friction factor of the jam underside.

f_o = composite friction factor of the flow under the jam.

F, F_1 = functions.

g = acceleration of gravity.

G, G_1 = functions.

h = depth of flow under the jam.

H = total depth of water = $h + t_s$.

H_g = total depth of water at location of grounding.

H_t = total depth of water at the toe of the jam.

K = dimensionless coefficient in seepage flow formula.

K_x = dimensionless coefficient defining the compressive strength of the jam.

m = exponent.

M_s = surface area per unit volume of particles of a porous medium.

p = porosity of jam.

q = flow dischage intensity under the jam.

q_p = flow discharge intensity through the voids of the jam.

q_T = total flow discharge intensity.

r = ratio of seepage discharge to discharge under the jam in equilibrium reach.

s_i = specific gravity of ice.

S_o = slope of channel bed.

S_w = slope of water surface.

t = ice jam thickness.

t_s = submerged portion of ice jam thickness.

u = flow velocity in the x-direction.

V = average flow velocity.

V_h = value of u at the ice jam underside.

W = width of channel.

x = downstream distance.

y = coordinate perpendicular to channel bed.

α = ratio of flow velocity at the ice jam underside to average flow velocity = V_h/V.

$\beta_1, \beta_2, \beta_3$ = dimensionless constants defining ice jam characteristics.

γ_w = unit weight of water.

γ_e = dimensional coefficient proportional to γ_w, as defined in Eq. 5.

ε = ratio of depth of flow under the jam to submerged portion of ice jam thickness in equilibrium reach.

η = dimensionless depth parameter.

θ = rate of change of slope of water surface with respect to thickness of submerged portion of ice jam in equilibrium reach.

λ = dimensional coefficient such that $\lambda\sqrt{S_w}$ = apparent seepage velocity.

μ = dimensionless coefficient defining ice jam characteristics.

ξ = dimensionless discharge parameter.

ρ = density of water.

σ_y = thickness-averaged, effective, stress in the jam in the y-direction.

τ_i = flow shear stress on jam underside

τ_b = flow shear stress on channel bed.

ϕ = angle of internal friction of jam.

ψ = rate of change of depth of flow under the jam with respect to thickness of submerged portion of ice jam in equilibrium reach.

APPENDIX III

Methods to Start Computation from Equilibrium Conditions

Simplified Method

It is assumed that (as outlined in main text):

$$S_w = S_o(h/h_e)^{-3} \tag{35}$$

and f_o = constant = f_{oe}. Then Eq. 1 may be re-written as

$$\frac{dt_s}{dx} = \beta_1 S_w\left[\beta_2 \frac{h}{t_s} + 1\right] - \beta_3 \frac{t_s}{W} = F \tag{36}$$

Moreover,

$$\frac{dh}{dx} = S_o - S_w - \frac{dt_s}{dx} \tag{37}$$

so that

$$\frac{dh}{dt_s} = \frac{S_o - S_w}{F} - 1 \tag{38}$$

Rearranging Eq. 38 and taking the limit at equilibrium gives

$$1 + \psi = \frac{0}{0} = \text{indeterminate} \tag{39}$$

Using L'Hospital's rule, we find

$$1 + \psi = -\left[\left(\frac{dS_w}{dt_s}\right)/\left(\frac{dF}{dt_s}\right)\right]_e \tag{40}$$

Differentiating Eqs. 35 and 36, and taking the limits at equilibrium gives

$$\left(\frac{dS_w}{dt_s}\right)_e = -\frac{3S_o}{h_e}\,\psi \tag{41}$$

$$\left(\frac{dF}{dt_s}\right)_e = -\frac{3\beta_1 S_o}{h_e}\,\psi\,(\beta_2\varepsilon + 1) + \frac{\beta_1 S_o}{t_{se}}\,\beta_2(\psi-\varepsilon) - \frac{\beta_3}{W} \tag{42}$$

in which $\varepsilon = h_e/t_{se}$. Noting that, at equilibrium, $F = 0$ (Eq. 36); solving for β_3/W; and substituting in Eq. 42 gives after some albegra

$$\left(\frac{dF}{dt_s}\right)_e = -\frac{\beta_1 S_o}{t_{se}}\left[\left(2\beta_2 + \frac{3}{\varepsilon}\right)\psi + (2\beta_2\varepsilon + 1)\right] \tag{43}$$

Substituting Eqs. 41 and 43 in Eq. 40 and re-arranging gives

$$\left(2\beta_2 + \frac{3}{\varepsilon}\right)\psi^2 + \left[\left(2\beta_2 + \frac{3}{\varepsilon}\right) + (1 + 2\varepsilon\beta_2) + \frac{3}{\varepsilon\beta_1}\right]\psi + (1 + 2\varepsilon\beta_2) = 0 \tag{44}$$

which has two negative roots. The root that is less than -1 should be chosen, as shown next. Equation 37 may be re-written as $dH/dx = S_o - S_w$. Since it is a physical requirement of the downstream transition that $dH/dx < 0$, S_w must exceed S_o. Moreover, writing Eq. 37 as

$$\frac{dt_s}{dx}\left(1 + \frac{dh}{dt_s}\right) = S_o - S_w \tag{45}$$

and noting that t_s has to increase with x (e.g., see Eq. 36), Eq. 45 suggests that $1 + (dh/dt_s) < 0$ which, taken to the limit at equilibrium, indicates that $\psi < -1$.

Detailed Method

From Eq. 40, we have

$$1+\psi = -\theta/\left(\frac{dF_1}{dt_s}\right)_e \tag{46}$$

in which $\theta = (dS_w/dt_s)_e$ and

$$F_1 = \frac{dt_s}{dx} = \beta_1 \left[\beta_2 \frac{f_o q^2}{4gh^2 t_s} + S_w\right] - \beta_3 \frac{t_s}{W} \tag{47}$$

Differentiating Eq. 47, substituting β_3/W as before, and taking the limit at equilibrium gives:

$$\left(\frac{dF_1}{dt_s}\right)_e = \beta_1 \left\{ \beta_2 S_o \varepsilon \left[\frac{1}{f_{oe}} \left(\frac{df_o}{dt_s}\right)_e + \frac{2}{q_e}\left(\frac{dq}{dt_s}\right)_e - \frac{2\psi}{h_e} - \frac{1}{t_{se}}\right] + \theta \right\} -$$

$$- \frac{\beta_1 S_o}{t_{se}} (\beta_2 \varepsilon + 1) \tag{48}$$

From Eq. 22:

$$\frac{1}{f_{oe}} \left(\frac{df_o}{dt_s}\right)_e = \frac{m}{t_{se}} \left(1 - \frac{\psi}{\varepsilon}\right) \tag{49}$$

From Eq. 13:

$$\frac{2}{q_e} \left(\frac{dq}{dt_s}\right)_e = - \frac{2r}{t_{se}} - \frac{r\theta}{S_o} \tag{50}$$

in which $r = q_{pe}/q_e$.

Substituting Eqs. 49 and 50 in Eq. 48 and re-arranging gives:

$$\left(\frac{dF_1}{dt_s}\right)_e = \frac{\beta_1 S_o}{t_{se}}\left[\frac{\theta t_{se}}{S_o}(1 - \beta_2\varepsilon r) - \beta_2\varepsilon(2-m+2r) - 1 - \beta_2(m+2)\psi\right] \quad (51)$$

Substituting Eq. 51 in Eq. 46 and solving for θ gives

$$\theta t_{se} = \beta_1 S_o(1+\psi)\frac{\beta_2\varepsilon(2+2r-m) + 1 + \beta_2(m+2)\psi}{1+\beta_1(1-\beta_2\varepsilon r)(1+\psi)} \quad (52)$$

which provides a first relationship between θ and ψ. Dividing Eq. 20 by Eq. 47 and re-arranging gives

$$\frac{dS_w}{dt_s} = \frac{2}{(2-\alpha)t_s}\left\{\frac{q\sqrt{S_w}}{\lambda h F_1}\left(\frac{f_o}{4} - \frac{S_w g h^3}{q^2}\right) - \frac{q\sqrt{S_w}}{\lambda h}\frac{dh}{dt_s} - (2-\alpha)S_w\right\} \quad (53)$$

Taking the limit at equilibrium and applying L'Hospital's rule to indeterminate terms gives

$$\frac{(2-\alpha)t_{se}\theta}{2} = \frac{S_o^{3/2} g h_e^2}{\lambda q_e}\frac{\left[\frac{d}{dt_s}\left(\frac{f_o q^2}{4gh^3 S_w}\right)\right]_e}{\left(\frac{dF_1}{dt_s}\right)_e} - \frac{q_e\sqrt{S_o}\psi}{\lambda h_e} - (2-\alpha)S_o \quad (54)$$

Letting

$$G = \frac{2-\alpha}{2}\theta t_{se} + \frac{q_e\sqrt{S_o}\psi}{\lambda h_e} + (2-\alpha)S_o \quad (55)$$

we obtain from Eq. 54:

$$G\left(\frac{dF_1}{dt_s}\right)_e = \frac{f_{oe}}{4}\frac{\sqrt{S_o}q_e}{\lambda h_e t_{se}}\left[m - 2r - \frac{\psi}{\varepsilon}(m+3) - \frac{\theta t_{se}}{S_o}(1+r)\right] \quad (56)$$

Substitution of Eq. 46 in Eq. 56 gives a second relationship between θ and ψ which after some algebra becomes

$$\frac{\theta t_{se}}{S_o}\left[1+r-\frac{4S_o}{f_{oe}}\frac{\psi}{1+\psi}-\frac{4\lambda h_e}{f_{oe}q_e}S_o^{3/2}(2-\alpha)\frac{G_1}{1+\psi}\right]=m-2r-\frac{\psi}{\varepsilon}(m+3) \quad (57)$$

in which

$$G_1 = 1+\frac{\theta t_{se}}{2S_o} \quad (58)$$

Combining Eqs. 52 and 57 results in a fourth-degree polynomial for ψ which can be solved implicitly. A simpler approach is to note that the third term within the brackets on the LHS of Eq. 57 is very small relative to other terms so that

$$\frac{\theta t_{se}}{S_o}\left(1+r-\frac{4S_o}{f_{oe}}\frac{\psi}{1+\psi}\right)\approx m-2r-\frac{\psi}{\varepsilon}(m+3) \quad (59)$$

which can be solved for θ and substituted in Eq. 52 to obtain a quadratic for ψ, i.e.:

$$A\psi^2+B\psi+C=0 \quad (60)$$

in which

$$A = \alpha_2\alpha_5+\frac{\alpha_3(m+3)}{\varepsilon\beta_1} \quad (61)$$

$$B = \alpha_2\alpha_4+\alpha_1\alpha_5-\frac{\alpha_3\alpha_6}{\beta_1}+\frac{(m+3)(1+\alpha_3)}{\varepsilon\beta_1} \quad (62)$$

$$C = \alpha_1\alpha_4-\frac{\alpha_6(1+\alpha_3)}{\beta_1} \quad (63)$$

with

$$\alpha_1 = \beta_2\varepsilon(2+2r-m) + 1 \tag{64}$$

$$\alpha_2 = \beta_2(m+2) \tag{65}$$

$$\alpha_3 = \beta_1(1-\beta_2\varepsilon r) \tag{66}$$

$$\alpha_4 = 1+r \tag{67}$$

$$\alpha_5 = 1+r-(4S_o/f_{oe}) \tag{68}$$

$$\alpha_6 = m-2r \tag{69}$$

The numerical algorithm is designed to calculate ψ from Eq. 60 and subsequently θ from Eq. 52. Then the neglected term in Eq. 57 is computed and compared to 1; if it is not negligible, a second iteration is performed and the process repeated until ψ and θ converge.

Finally, it is noted that the assumptions made for the simplified method are equivalent to setting $m = r = 0$ and $4S_o/f_{oe} \ll 1$ so that $\alpha_1 = 2\beta_2\varepsilon + 1$, $\alpha_2 = 2\beta_2$, $\alpha_3 = \beta_1$, $\alpha_4 = 1$, $\alpha_5 = 1$ and $\alpha_6 = 0$. Substitution of these values in Eqs. 61-63 gives identical coefficients of the quadratic as those found under the simplified method.

APPENDIX IV

Approximate Calculation of H_g

To express t_s as an approximate function of h, let a polynomial form be assumed, i.e.:

$$t_s = H_g + b_1 h + b_2 h^2 + b_3 h^3 \tag{70}$$

which satisfies the condition: $h = 0$, $t_s = H_g$ (grounding). Eq. 70 gives

$$\frac{dt_s}{dh} = b_1 + 2b_2 h + 3b_3 h^2 \tag{71}$$

$$\frac{d^2 t_s}{dh^2} = 2b_2 + 6b_3 h \tag{72}$$

Applying Eq. 71 at equilibrium gives one equation between b_1, b_2 and b_3 (as has been found before, $(dt_s/dh)_e = 1/\psi$). Two additional equations can be obtained by considering conditions at the point of grounding, as follows.

In Eq. 1, it may be noted that the term $\beta_2 f_o q^2/4gh^2 t_s$ represents the relative contribution of τ_i to the forces applied on the jam. As the point of grounding is approached, τ_i becomes negligible relative to the downslope component of the jam's own weight per unit area. Hence

$$\left(\frac{dt_s}{dx}\right)_{x \to x_g} \approx \beta_1 S_w - \beta_3 \frac{t_s}{W} \tag{73}$$

Moreoever, S_o becomes negligibly small relative to S_w near the point of grounding. Eq. 21 then reduces to:

$$\left(\frac{dh}{dx}\right)_{x\to x_g} = -S_w - \left(\frac{dt_s}{dx}\right)_{x\to x_g} \tag{74}$$

From the results of the numerical solution, it has been found that $\beta_1 S_w \gg \beta_3 (t_s/W)$ when grounding is approached. Therefore, Eqs. 73 and 74 reduce further to:

$$\left(\frac{dt_s}{dx}\right)_{x\to x_g} = \beta_1 S_w \tag{75}$$

$$\left(\frac{dh}{dx}\right)_{x\to x_g} = -(1+\beta_1)S_w \tag{76}$$

Dividing Eq. 75 by Eq. 76 gives

$$\left(\frac{dt_s}{dh}\right)_{x\to x_g} = -\frac{\beta_1}{1+\beta_1} \tag{77}$$

and, from Eq. 77:

$$\left(\frac{d^2t_s}{dh^2}\right)_{x\to x_g} = 0 \tag{78}$$

Eqs. 77 and 78 are the two additional relationships needed to determine the coefficients b_1, b_2 amd b_3 (see Eqs. 71 and 72). The result is:

$$b_1 = -\frac{\beta_1}{1+\beta_1} \tag{79}$$

$$b_2 = 0 \tag{80}$$

$$b_3 = \frac{1}{3h_e^2}\left(\frac{1}{\psi} + \frac{\beta_1}{1+\beta_1}\right) \tag{81}$$

Substituting Eqs. 79-81 in Eq. 70 and applying the latter to equilibrium conditions gives

$$t_{se} = H_g - \frac{h_e}{3}\left(\frac{2\beta_1}{1+\beta_1} + \frac{1}{|\psi|}\right) \tag{82}$$

which is equivalent to Eq. 33. It is important to note that in this application, the actual value of ψ must be used, i.e., ψ should be determined by the detailed method as outlined in Appendix III.

TABLE 1. Variation of Coefficients K_x, β_1 and β_3 with K_1 and ϕ. ($\mu = 1.20$, $p = 0.40$)

K_1	$\phi(^\circ)$	K_x	β_1	β_3
0	90.00	0	0	0
0.10	58.28	12.3729	1.5491	0.1616
0.20	51.17	8.0502	2.3809	0.2484
0.30	46.58	6.3082	3.0384	0.3171
0.40	43.16	5.3299	3.5961	0.3753
0.50	40.44	4.6924	4.0847	0.4262
0.60	38.18	4.2374	4.5232	0.4720
0.70	36.26	3.8954	4.9204	0.5134
0.80	34.59	3.6264	5.2853	0.5515
0.90	33.11	3.4077	5.6245	0.5869
1.00	31.80	3.2279	5.9378	0.6196

TABLE 2. Summary of Predicted Parameters. Thames River.
W = 109m, S_o = .00027, μ = 1.20, s_i = 0.92, p = 0.4, α = 0.0

q_T (m^3/s)	H_e	t_{se}	H_o	t_{so}	$f_i/2f_o$	K_x	λ (m/s)	x_g	H_g	S_{wg}	$\overline{S_w}$ * 50	100	200
3.09	5.40	1.03	5.37	1.04	0.625	4.32	.75	957	4.71	.76891	.01033	.00587	.00328
3.09	5.40	1.03	5.37	1.04	0.625	4.32	1.0	970	4.70	.43479	.01008	.00571	.00324
3.09	5.38	1.03	5.36	1.04	0.625	4.32	2.0	1024	4.68	.11130	.00991	.00550	.00320
3.09	5.37	1.03	5.34	1.04	0.625	4.32	3.0	1079	4.64	.05018	.00982	.00572	.00330
3.09	5.36	1.03	5.33	1.04	0.625	4.32	4.0	1138	4.60	.02833	.00966	.00587	.00341
3.09	5.34	1.03	5.31	1.04	0.625	4.32	5.0	1200	4.56	.01863	.00937	.00577	.00342
3.09	5.40	1.03	5.37	1.04	0.625	3.228	.75	740	4.86	.61436	.00812	.00461	.00274
3.09	5.40	1.03	5.37	1.04	0.625	6.0	.75	1253	4.50	.83691	.01261	.00702	.00400
3.09	5.40	1.03	5.37	1.04	0.625	8.0	.75	1562	4.30	.92024	.01531	.00846	.00479
3.09	5.40	1.03	5.37	1.04	0.625	10.0	.75	1835	4.13	1.00848	.01738	.01007	.00555
3.09	5.38	1.03	5.35	1.04	0.625	3.228	2.00	800	4.82	.10315	.00819	.00469	.00269
3.09	5.38	1.03	5.35	1.04	0.625	6.0	2.00	1328	4.47	.12117	.01216	.00713	.00405
5.09	5.38	1.03	5.35	1.04	0.625	8.0	2.00	1645	4.26	.13263	.01481	.00876	.00490
3.09	5.38	1.03	5.35	1.04	0.625	10.0	2.00	1924	4.09	.14487	.01640	.00918	.00532
3.09	5.34	1.03	5.31	1.04	0.625	3.228	5.00	956	4.72	.01753	.00786	.00495	.00289
3.09	5.34	1.03	5.31	1.04	0.625	6.0	5.00	1528	4.35	.02036	.01127	.00700	.00419
3.09	5.34	1.03	5.31	1.04	0.625	8.0	5.00	1863	4.15	.02248	.01305	.00815	.00477
3.09	5.34	1.03	5.31	1.04	0.625	10.0	5.00	2156	3.98	.02442	.01443	.00934	.00550
3.09	4.72	.74	4.69	.75	0.300	3.228	.75	722	4.15	.84813	.00865	.00476	.00252
3.09	4.72	.784	4.69	.75	0.300	6.0	.75	1221	3.80	1.17651	.01296	.00731	.00381
3.09	4.72	.74	4.69	.75	0.300	10.0	.75	177	3.43	1.45215	.01850	.01011	.00613
3.09	5.68	1.16	5.65	1.17	0.800	3.228	.75	731	5.15	.61172	.00813	.00449	.00257
3.09	5.68	1.16	5.65	1.17	0.800	6.0	.75	1242	4.60	.73977	.01256	.00694	.00394
3.09	5.68	1.16	5.65	1.17	0.800	10.0	.75	1828	4.41	.87360	.01706	.00980	.00547
.50	2.32	0.70	2.30	.71	0.625	4.32	.75	295	2.06	.10788	.00407	.00263	.00151
1.00	3.17	.80	3.15	.82	0.625	4.32	.75	457	2.78	.23020	.00643	.00356	.00194
2.00	4.38	.93	4.35	.95	0.625	4.32	.75	714	3.83	.48599	.00836	.00456	.00253
4.00	6.13	1.09	6.10	1.10	0.625	4.32	.75	1146	5.33	.85650	.01142	.00665	.00369
5.00	6.84	1.15	6.81	1.16	0.625	4.32	.75	1348	5.93	1.10694	.01293	.00736	.00410
5.00	2.32	0.70	2.30	.71	0.625	8.00	.75	487	1.90	.12542	.00684	.00417	.00226
1.00	3.17	0.80	3.15	.82	0.625	8.00	.75	756	2.56	.27312	.00965	.00528	.00284
2.00	4.38	0.93	4.35	.95	0.625	8.00	.75	1175	3.51	.58324	.01333	.00723	.00437
4.00	6.13	1.09	6.10	1.10	0.625	8.00	.75	1856	4.86	1.20698	.01729	.01003	.00553
5.00	6.84	1.15	6.81	1.16	0.625	8.00	.75	2161	5.40	1.52344	.01940	.01063	.00599

* Average water surface slope over last 50, 100 and 200 m of jam stage profile

TABLE 3. Summary of Predicted Parameters. Athabasca River.
$W = 560m$, $S = .00036$, $\mu = 1.20$, $s_i = 0.92$, $p = 0.4$, $\alpha = 0.0$

q_T (m^3/s)	H_e	t_{se}	H_o	t_{so}	$f_i/2f_o$	K_x	λ (m/s)	x_g	H_g	S_{wg}	$\overline{S_w}$ 50	100	200
.50	5.04	2.85	5.03	2.89	.625	4.32	.75	559	4.67	.02074	.00540	.00328	.00193
1.00	6.34	3.15	6.33	3.18	.625	4.32	.75	800	5.81	.05300	.00764	.00453	.00268
2.00	8.15	3.52	8.14	3.55	.625	4.32	.75	1164	7.39	.13124	.01059	.00597	.00352
3.00	9.52	3.77	9.51	3.80	.625	4.32	.75	1454	8.59	.21708	.01296	.00745	.00422
4.00	10.68	3.97	10.67	4.00	.625	4.32	.75	1703	9.61	.30964	.01488	.00848	.00477
5.00	11.78	4.14	11.69	4.14	.625	4.32	.75	1926	10.49	.40435	.01617	.00929	.00541
.50	5.04	2.85	5.02	2.89	.625	8.00	.75	906	4.44	.02264	.00819	.00485	.00269
1.00	6.34	3.15	6.33	3.18	.625	8.00	.75	1307	5.48	.05938	.01085	.00670	.00390
2.00	8.15	3.52	8.13	3.55	.625	8.00	.75	1912	6.92	.14846	.01554	.00890	.00519
3.00	9.52	3.77	9.51	3.80	.625	8.00	.75	2393	8.04	.25059	.01822	.01064	.00610
4.00	10.68	3.97	10.67	4.00	.625	8.00	.75	2808	8.95	.35677	.02159	.01240	.00715
5.00	11.70	4.14	11.69	4.14	.625	8.00	.75	3178	9.75	.46817	.02378	.01368	.00789
2.00	8.15	3.52	8.14	3.55	.625	3.228	.75	903	7.55	.12493	.00890	.00498	.00294
2.00	8.15	3.52	8.14	3.55	.625	6.0	.75	1528	7.16	.13897	.01314	.00776	.00446
2.00	8.15	3.52	8.13	3.55	.625	8.0	.75	1912	6.92	.14846	.01554	.00890	.00579
2.00	8.15	3.52	8.13	3.54	.625	10.0	.75	2253	6.73	.15802	.01759	.00989	.00581
2.00	8.02	3.50	8.01	3.53	.625	3.228	2.00	1035	7.43	.01852	.00750	.00468	.00280
2.00	8.02	3.50	8.01	3.52	.625	4.32	2.00	1323	7.25	.01905	.00908	.00571	.00344
2.00	8.02	3.50	8.01	3.52	.625	6.00	2.00	1720	7.03	.02036	.01081	.00688	.00419
2.00	8.02	3.50	8.00	3.52	.625	8.0	2.00	2136	6.80	.02176	.01246	.00801	.00497
2.00	8.02	3.50	8.00	3.52	.625	10.0	2.00	2502	6.60	.02310	.01374	.00891	.00544
2.00	7.70	3.43	7.70	3.47	.625	3.228	5.00	1470	7.06	.00332	.00345	.00323	.00251
2.00	7.70	3.43	7.69	3.46	.625	4.32	5.00	1842	6.90	.00347	.00360	.00347	.00283
2.00	7.70	3.43	7.69	3.46	.625	6.0	5.00	2336	6.70	.00372	.00382	.00372	.00316
2.00	7.70	3.43	7.69	3.46	.625	8.0	5.00	2852	6.44	.00388	.00402	.00400	.00333
2.00	7.70	3.43	7.69	3.46	.625	10.0	5.00	3284	6.26	.00412	.00426	.00423	.00375

TABLE 4. Comparison of H_t with H_g, Thames River Example.

q_T (m^2/s)	H_t (m)	H_g (m)	
		K_x = 4.32	K_x = 8.00
0.5	1.69	2.06[g]	1.90[g]
1.0	2.37	2.78[g]	2.56[g]
2.0	3.40	3.83[g]	3.51[g]
3.09	4.30	4.71[g]	4.30[g]
4.0	4.96	5.33[g]	4.86[f]
5.0	5.62	5.93[g]	5.40[f]
6.0	6.22	6.47[g]	5.90[f]

g = grounded toe;

f = floating toe.

TABLE 5. Comparison of H_t with H_g, Athabasca River example.

q_T (m^2/s)	H_t (m)	H_g (m)	
		$K_x = 4.32$	$K_x = 8.00$
0.5	1.98	4.67^g	4.44^g
1.0	2.57	5.81^g	5.48^g
2.0	3.46	7.39^g	6.92^g
3.0	4.19	8.59^g	8.04^g
4.0	4.82	9.61^g	8.95^g
5.0	5.32	10.49^g	9.75^g

TABLE 6. Test of Approximate H_g - Eq. 33

Value of m	$\frac{1}{\lvert\psi\rvert}$	$\frac{\beta_1}{1+\beta_1}$	Approx. Hg (m)	Calc'd Hg (m)	% Error
1.17	.7247	.7616	4.31	4.51	-4.43
1.17	.7247	.7616	4.31	4.46	-3.36
1.17	.8364	.8161	7.32	7.40	-1.08
1.17	.8364	.8161	7.32	7.39	-0.95
1.17	.8716	.8559	7.47	7.51	-0.53
1.17	.8706	.8559	8.62	8.68	-0.69
1.17	.8696	.8559	9.58	9.67	-0.93
1.17	.8357	.8161	8.85	8.94	-1.01
1.17	.8385	.8161	8.75	8.80	-0.57
1.17	.8447	.8161	8.49	8.44	0.59
1.17	.7899	.7616	7.08	7.15	-0.98
1.17	.7893	.7616	8.14	8.24	-1.21
1.17	.7885	.7616	9.02	9.15	-1.42
1.17	.6996	.6571	6.65	6.73	-1.19
1.17	.6999	.6571	7.61	7.73	-1.55
1.17	.6997	.6571	8.41	8.56	-1.75
1.17	.8715	.8559	9.60	9.65	-0.52
1.17	.8711	.8559	10.58	10.66	-0.75
1.17	.8706	.8559	11.44	11.53	-0.78
1.17	.8363	.8161	10.56	10.65	-0.85
1.17	.8396	.8161	10.41	10.46	-0.48
1.17	.8471	.8161	10.04	9.96	0.80
1.17	.7893	.7616	9.13	9.21	-0.87
1.17	.7892	.7616	10.03	10.13	-0.99
1.17	.7890	.7616	10.82	10.94	-1.10
1.17	.6983	.6571	8.61	8.71	-1.15
1.17	.6988	.6571	9.43	9.55	-1.26
1.17	.6991	.6571	10.14	10.29	-1.46
1.0	.7369	.8559	4.88	5.10	-4.31
0.8	.6085	.8559	5.04	5.39	-6.49
0.6	.4725	.8559	5.21	5.64	-7.62
1.0	.6254	.7055	4.24	4.51	-5.99
0.8	.5365	.7055	4.41	4.74	-6.96
0.6	.4364	.7055	4.59	4.96	-7.46
1.0	.8659	.8559	7.56	7.61	-0.66
0.8	.8582	.8559	7.63	7.68	-0.65
0.6	.8476	.8559	7.70	7.75	-0.65
1.0	.7350	.7055	6.89	6.98	-1.29
0.8	.7251	.7055	6.94	7.03	-1.28
0.6	.7124	.7055	7.00	7.08	-1.13

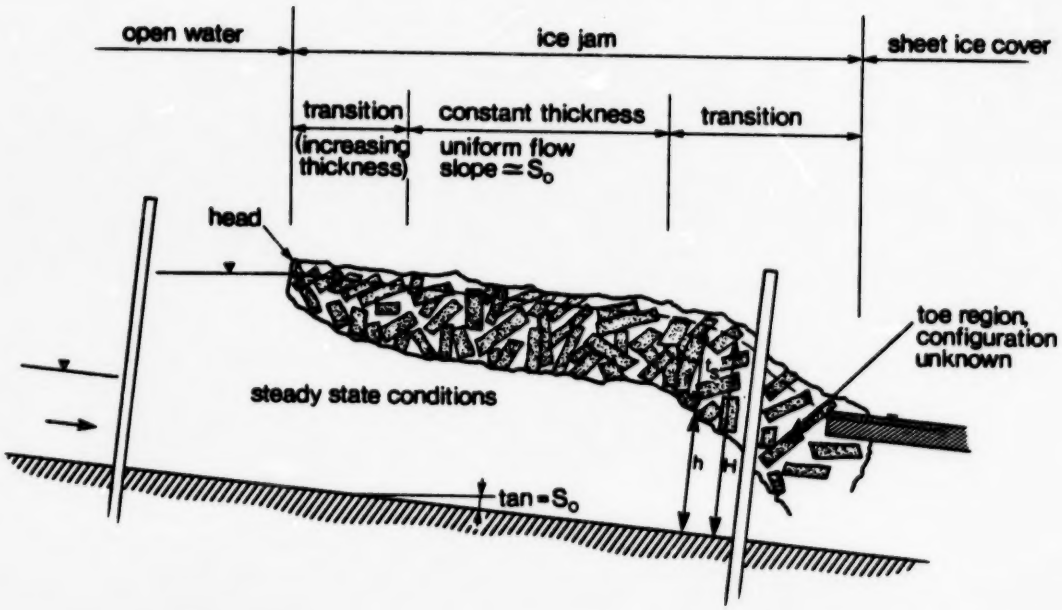

Fig. 1. Schematic Illustration of an Equilibrium Jam

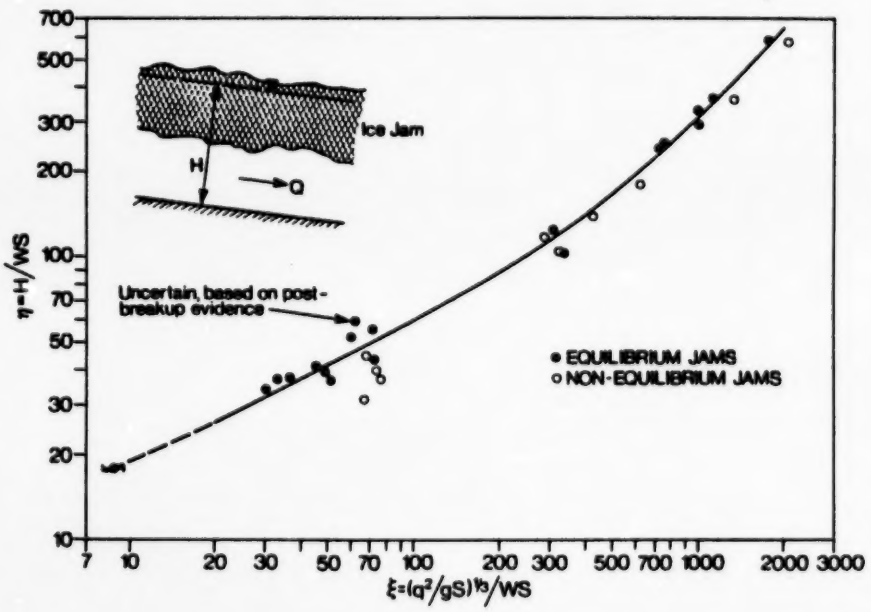

Fig. 2. Dimensionless Depth Versus Dimensionless Discharge for Breakup Jams

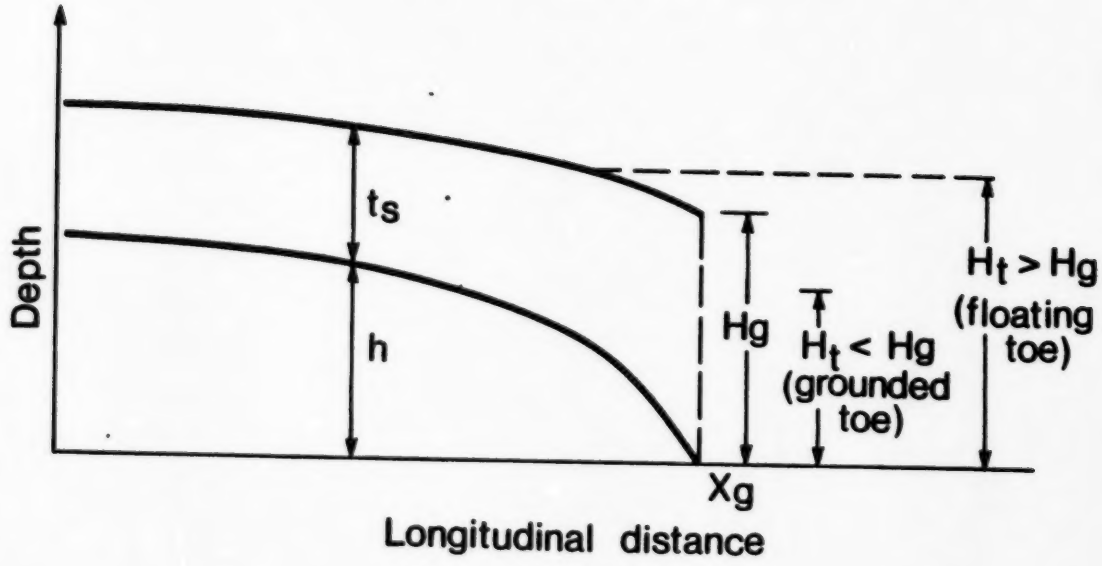

Fig. 3. Schematic Illustration of Toe Conditions

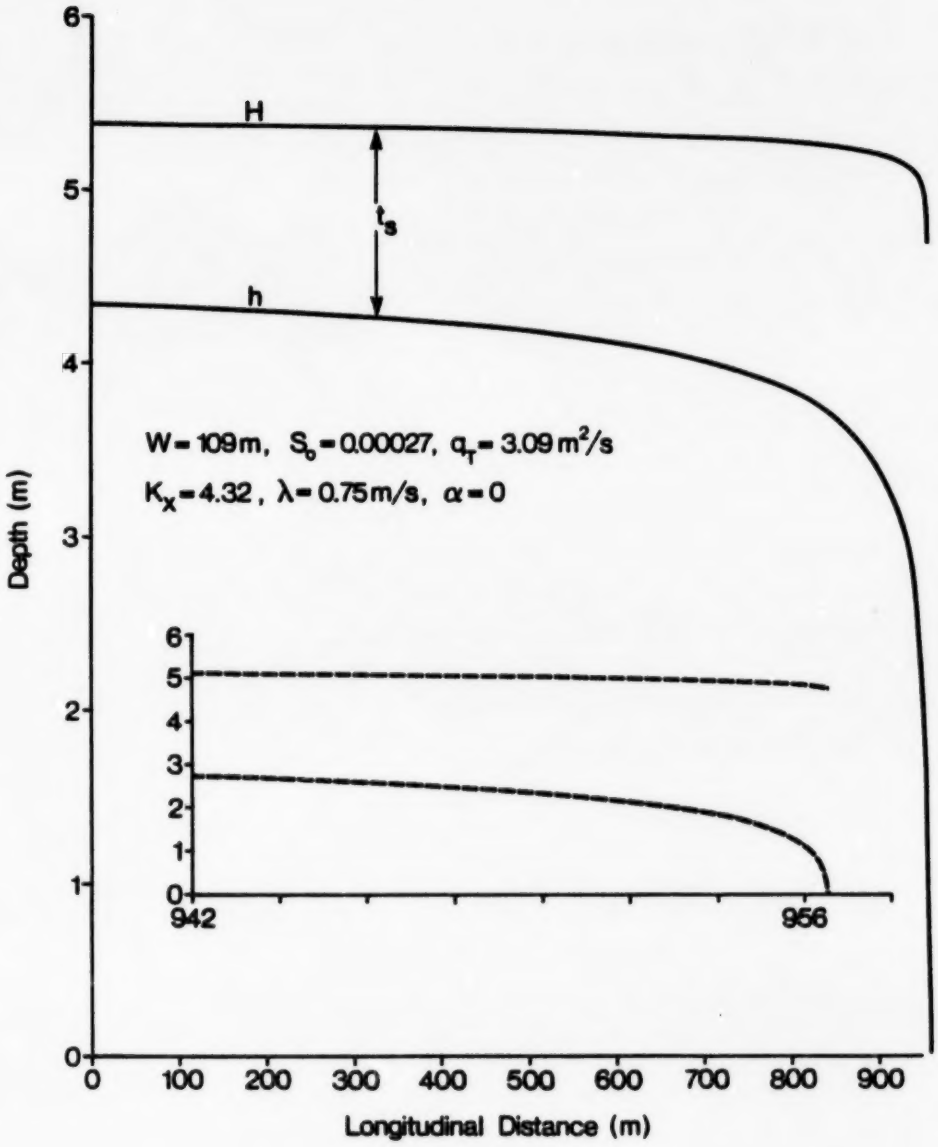

Fig. 4. Computed Ice Jam Profile for Thames River Example
Insert Shows Profile in the Vicinity of Grounding, Plotted Without Distortion

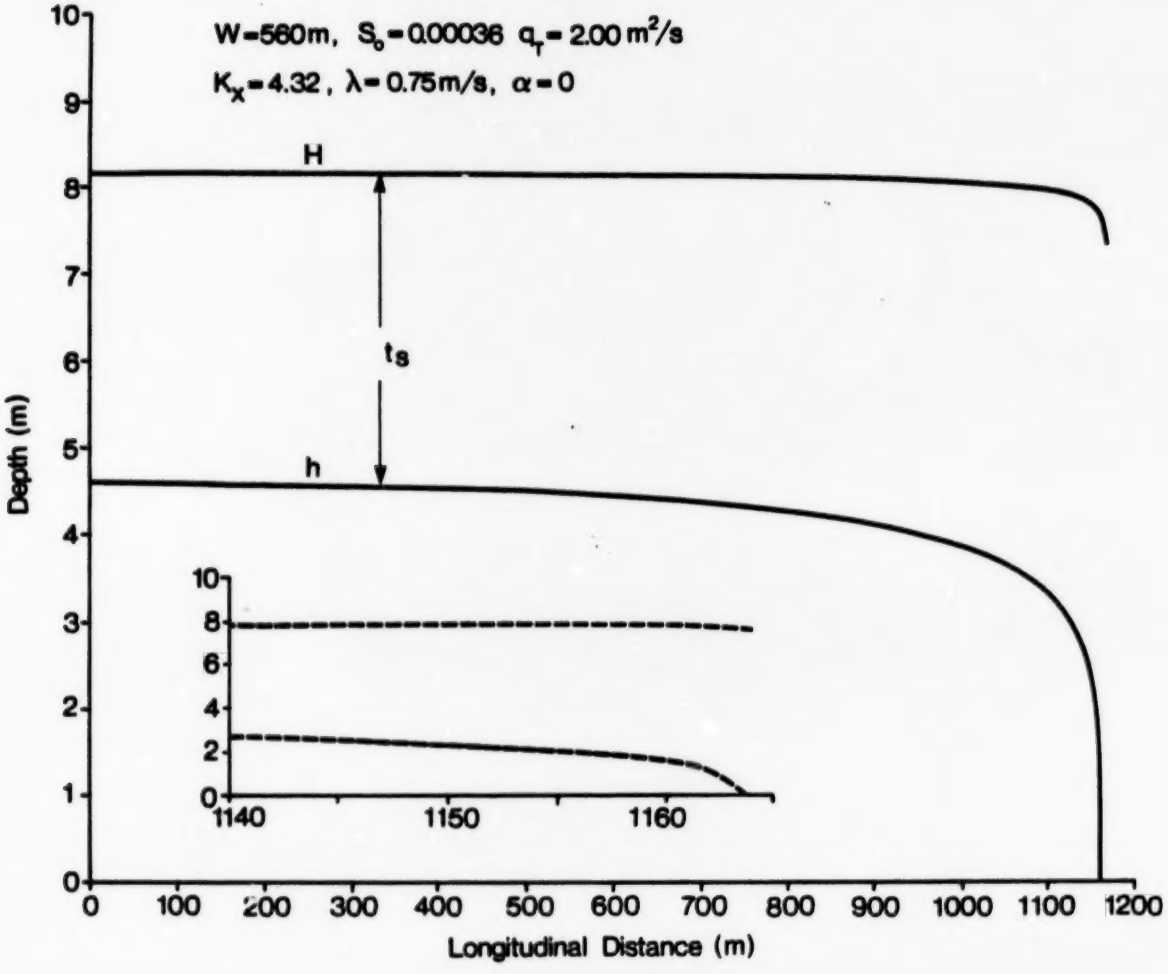

Fig. 5. Computed Ice Jam Profile for Athabasca River Example. Insert Shows Profile in the Vicinity of Grounding, Plotted Without Distortion

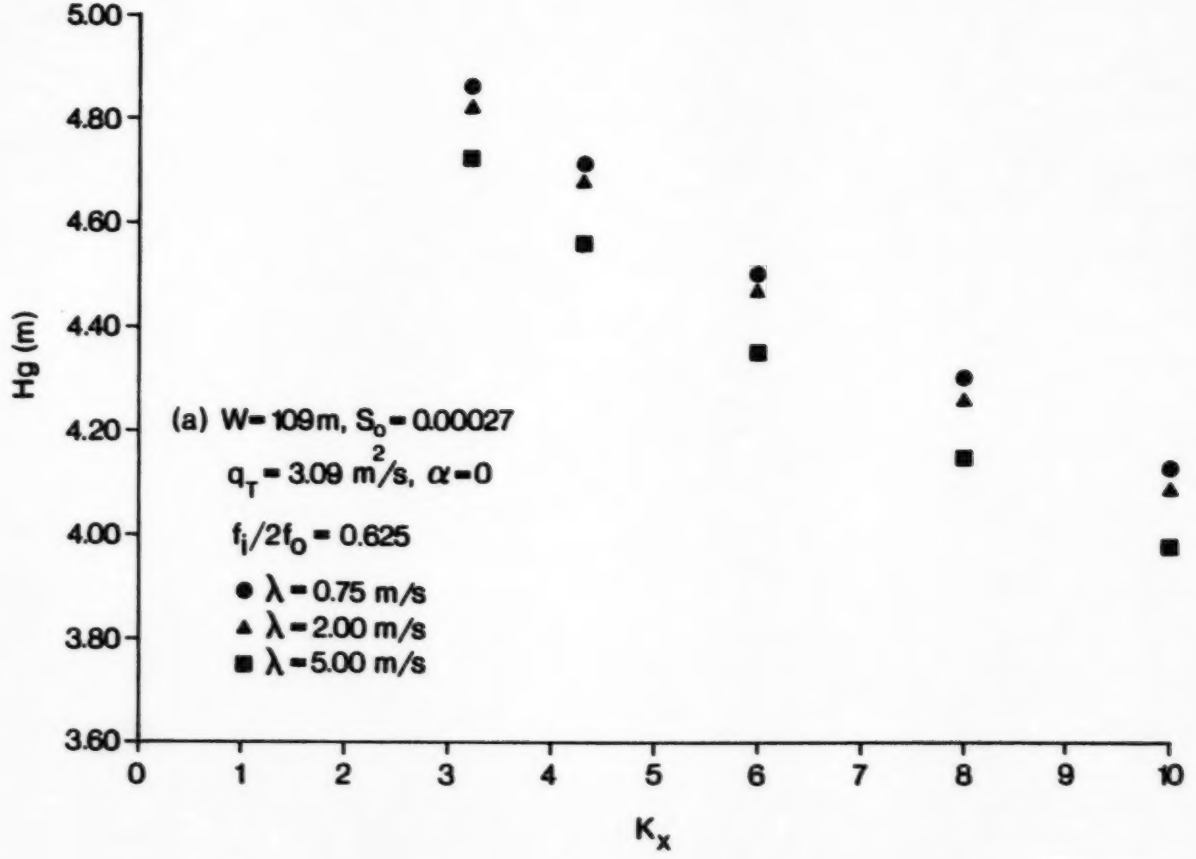

Fig. 6. Effects of k_x and λ on Hg, Thames River Example

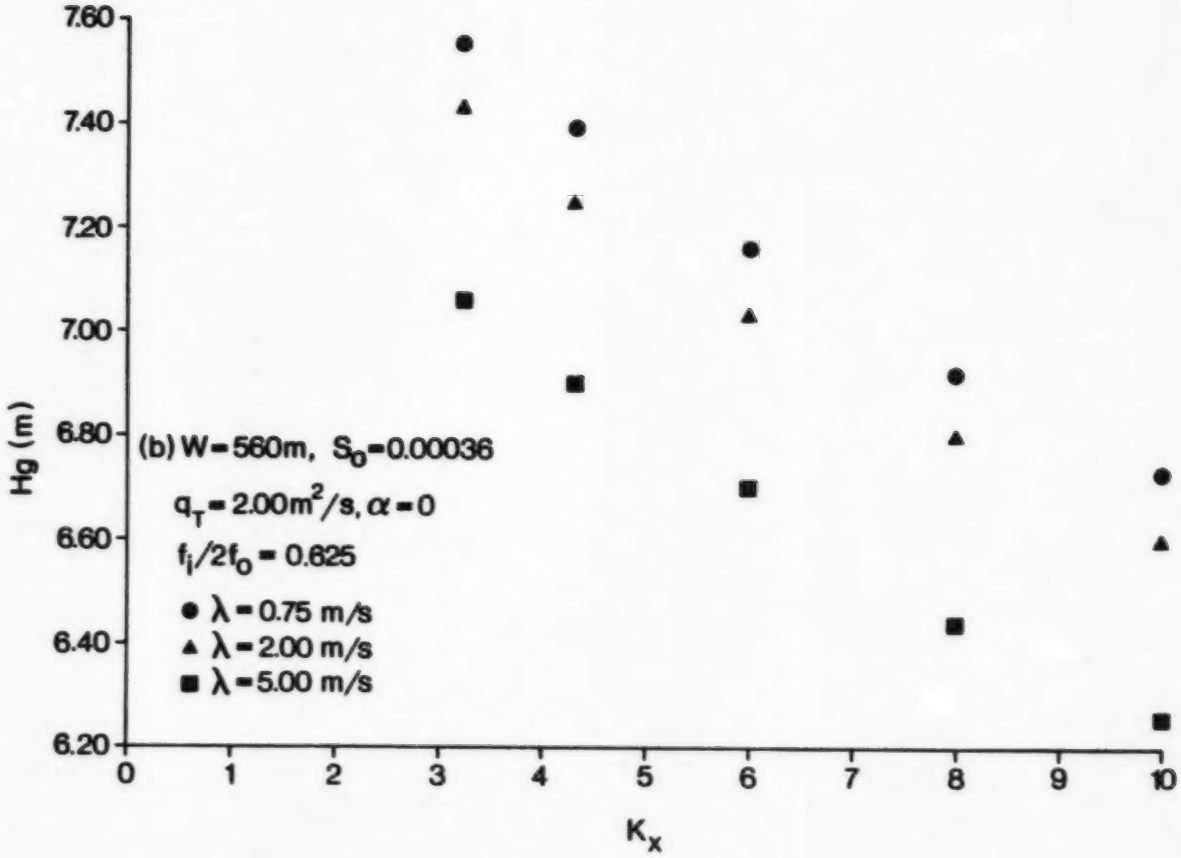

Fig. 6. Effects of k_x and λ on Hq, Athabasca River Example

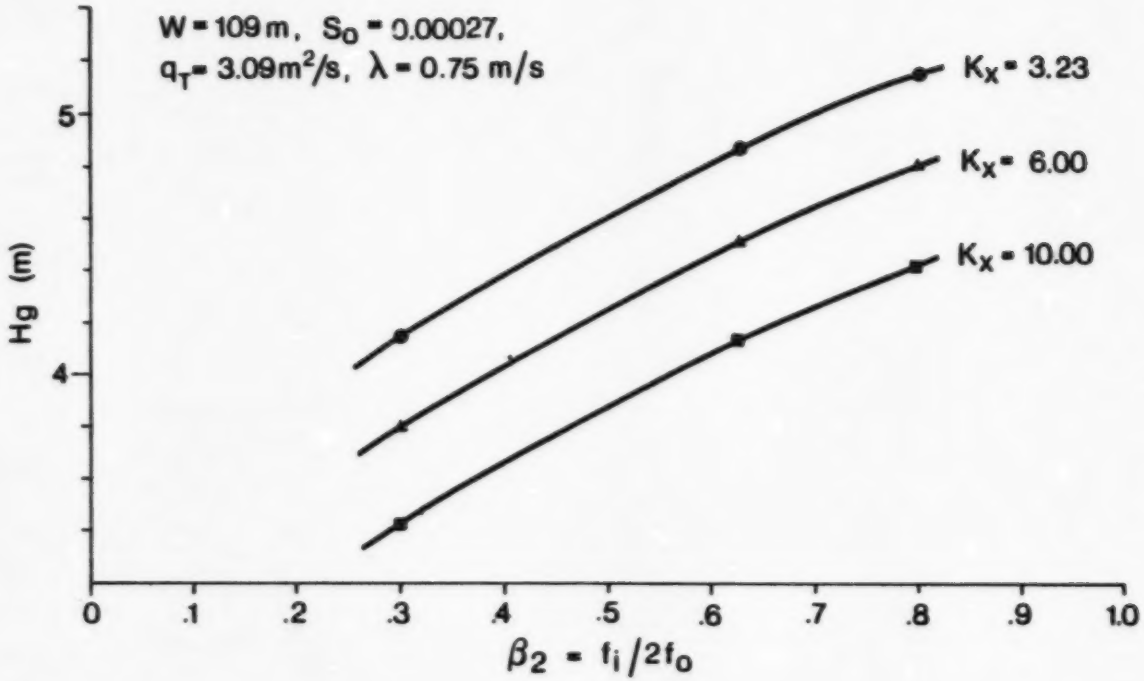

Fig. 7. Effects of $f_i/2f_o$ on Hg, Thames River Example

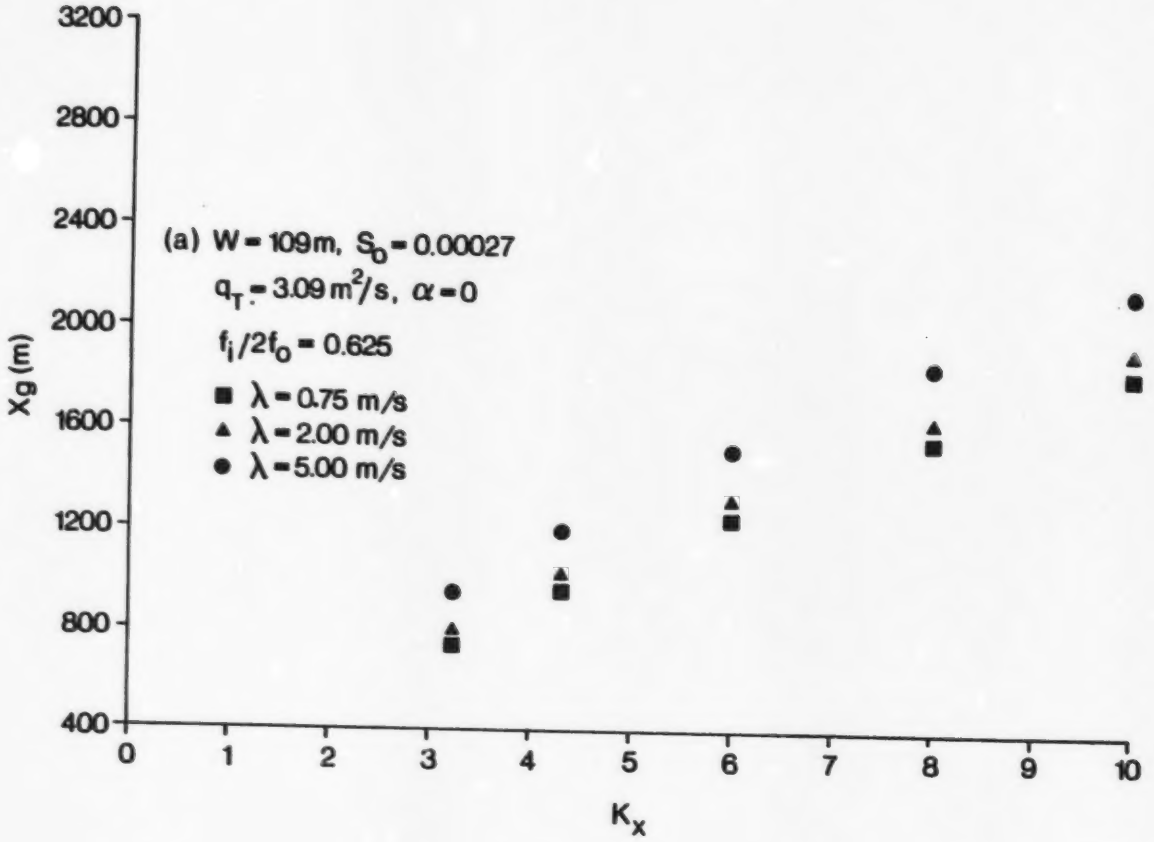

Fig. 8. Effects of k_x and λ on x_g, Thames River Example

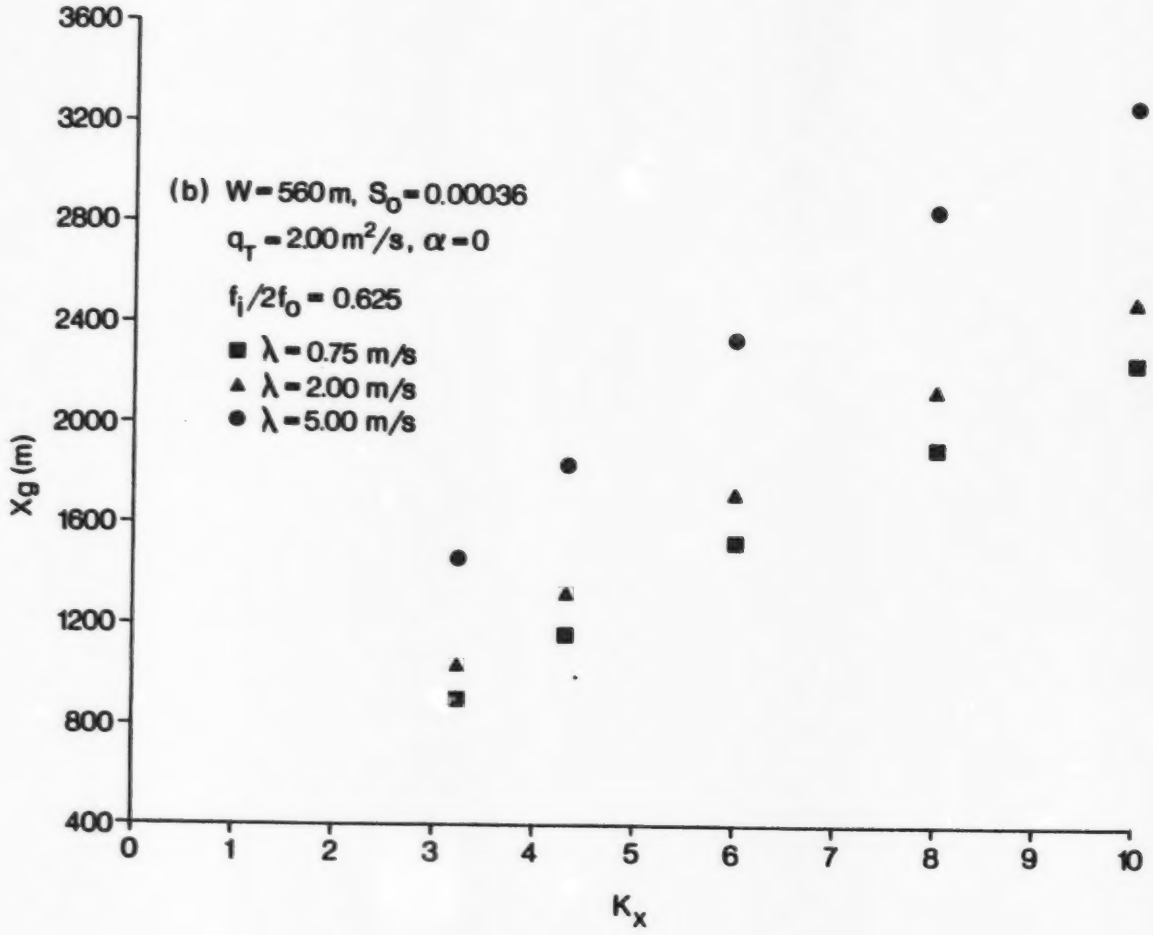

Fig. 8. Effects of k_x and λ on x_g, Athabasca River Example

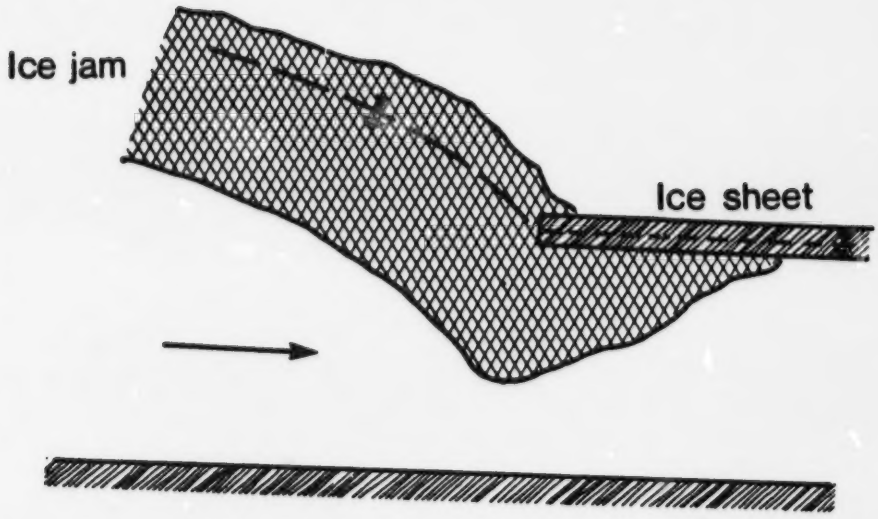

Fig. 9. Probable Configuration of Floating Toe

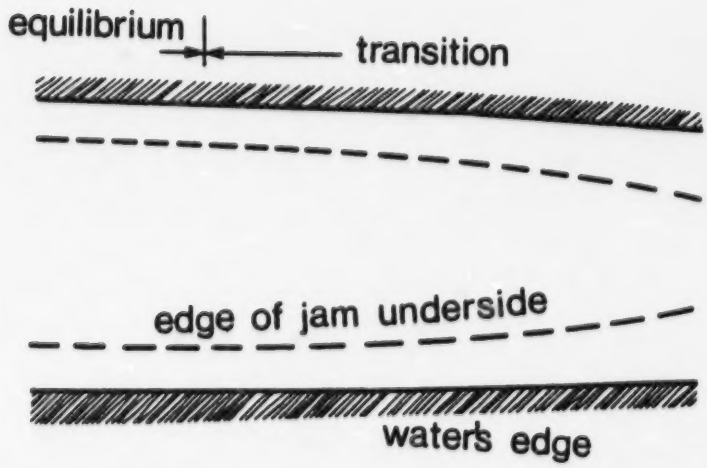

Fig. 10. Plan View of Jammed River with Non-Rectangular Cross-Section